Direct Electroplating on Indium-Tin-Oxide-coated Textured and Polished Silicon Substrates via Transition Metal Alloyed Interlayers

Jochen Politze,*,† Stefan Scholz,† Horst Windgassen,† Christian Schmitz,† Kaining Ding,‡ Weiyuan Duan,‡ and Joachim Knoch†

Institute of Semiconductor Electronics IHT, RWTH Aachen University, Sommerfeldstr. 18, 52074 Aachen, Germany, and Institute of Energy and Climate Research IEK-5 Photovoltaics, Forschungszentrum Jülich, 52425 Jülich, Germany

E-mail: politze@iht.rwth-aachen.de

Abstract

In this study Fe electroplating is used on polished or pyramidally textured indium-tin-oxide (ITO)-coated silicon substrates as an initial layer for subsequent Ni and Cu plating. Up to 15 µm thick Cu layers are deposited on the Ni/Fe intermediate layer. The adhesion strength of this metal layer stack is qualitatively shown by the scotch tape method and quantified by measuring the pull-off stress of the metal stack on ITO. 1.44 MPa and 1.28 MPa have to be applied to pull off the metal stack from polished and pyramidally textured substrates, respectively. Electrical contact properties are

*To whom correspondence should be addressed
†IHT
‡IEK-5

measured by circular transmission line model (CTLM) structures. Very low contact resistivity for electroplated metal on ITO of $6.5 \times 10^{-7}\,\Omega\,\mathrm{cm}^2$ and $9.0 \times 10^{-7}\,\Omega\,\mathrm{cm}^2$ with transfer lengths of 487 nm and 720 nm are determined for polished and pyramidally textured substrates, respectively.

Introduction

A transparent conductive oxide (TCO) is a material combining high electrical conductivity and a high transmission coefficient of light. One of the most commonly used TCOs is indium-tin-oxide (ITO) providing an electrical contact in solar cell and display applications. An additional metal layer is usually deposited to contact the ITO and reduce series resistances. To increase solar cell efficiency or display size, many efforts have been undertaken to reduce the metal sheet resistance and metal/ITO contact resistance while maintaining low production cost and high throughput. Silver screen printing with subsequent annealing is a low-cost technology used for applying metal grids on solar cells. However, the screen printed layers have a relatively low bulk conductivity. Therefore, alternative techniques for the metal contact deposition have been investigated. In particular, Cu electroplating appears promising since electroplated Cu has higher bulk conductivity than screen printed silver. Additionally, Cu has a higher availability and is thus cheaper than silver. Electroplating provides low processing temperatures and is a low-cost technology. Although direct Cu electroplating on ITO sounds compelling, these Cu layers show poor adhesion which may negatively influence the contact resistance and lead to the detachment of the metal layer from the substrate.

Several studies have investigated surface treatments to improve metal adhesion to different TCOs. Liu et al.[1] used electrolysis reduction changing the valency of the surface of tin oxide. Kim and Cha[2] worked with Sn-sensitization and Pd-activation for electroless Cu plating on ITO. Hau et al.[3] employed a combination of coating the ITO surface with a monolayer of 3-mercaptopropyl-trimethoxysilane (MPS) and a sweeping potential technique

to increase nucleation rate and adhesion of electroplated silver. Initially evaporated Cu seed layers with subsequent electroplating were also shown to have good adhesion.[4–6] However, the metal evaporation technique needs a high vacuum chamber and does not provide high-throughput.

Ahmet et al.[7] invented a process where samples partially coated with metal oxides, e.g. ITO, are immersed into an electrolyte containing a wetting agent and a metal salt such as iron sulfate. By the subsequent addition of a reduction agent, the electron transfer agent is reduced and an adherent metal layer is deposited on the metal oxide. Recently, electroplating of intermediate transition metal layers before the Cu electroplating were studied. Lee et al.[8] used an electroplated Cu-Ni alloy seed layer. Minsek[9] invented a process where the electroplating of zinc, zinc oxide and zinc alloys leads to adherent films on TCOs. After zinc deposition, an intermediate zinc oxide layer forms at the boundary of zinc and the TCO due to the low redox potential of zinc leading to a strongly bonded metal layer. Furthermore, it is hypothesized that Fe and Cr, due to their low redox potential, may also form oxides on the surface of a TCO after electroplating and potentially show good adhesion. However, this has not been demonstrated experimentally prior to this study.

In this work Cu electroplating on ITO-coated polished or pyramidally textured Si substrates is investigated by means of an adhesion-promoting electroplated Fe/Ni interlayer. Samples with circular transmission line model (CTLM) structures were fabricated to determine the contact resistivity of the metal stack on ITO. The adhesion strength of the metal stack was verified by scotch tape method and by measuring the pull-off force of the metal stack on the ITO. To the best of our knowledge, this is the first reported investigation of direct Fe electroplating on ITO. It is also the first study of the Fe/ITO interface where its adhesion strength by means of measuring the pull-off force is quantified and its contact resistivity is determined.

Experimental Section

The following chemicals were used as electrolyte compounds or for the anode preparation: NB Semiplate Ni 100 (NB Technologies GmbH), iron(II) sulfate heptahydrate (p. A., CAS 7782-63-0), L-ascorbic acid (food-grade), boric acid (>99.5%, CAS 10045-35-3), copper(II) pyrophosphate hydrate (CAS 16570-28-8), potassium pyrophosphate (97%, CAS 7320-34-5), ammonium nitrate (>99%, CAS 6484-52-2), ammonium oxalate monohydrate (>99%, CAS 6009-70-7), sulfuric acid (96%). Samples were structurized with Photoresist AZ12XT-20PL-10 (Microchemicals GmbH) by means of UV-exposure with a LaserWriter (LW405C, Microtech s.r.l.) and a mask aligner (MA6, SÜSS MicroTec SE). Adhesion promoter hexamethyldisilazane (HMDS) (Microchemicals GmbH, CAS 999-97-3) was employed for the photoresist on the substrates with an HMDS coater (QS V 200 BM, solar-semi GmbH) and exposed features of the photoresist were developed with AZ 826 MIF (Microchemicals GmbH). A programmable power supply HMP 4040 (HAMEG GmbH) was employed for electroplating. Micrographs were taken with a scanning electron microscope (SEM) (Zeiss Sigma, Carl Zeiss Microscopy Deutschland GmbH). A parameter analyzer Keithley 4200A-SCS (Tektronix GmbH) was utilized in combination with a 4-point-measurement setup to perform I-V-measurements. Measured data is evaluated with MATLAB R2021a.

Substrates

Double-side polished Si (Siegert Wafer GmbH, float-zone, Ph-doped, n-type, <100>, 1–5 Ωcm, diameter 100 mm, thickness 280(20) µm) and Si wafers (LONGi Green Energy Technology Co., Ltd., Czochralski grown, Ph-doped, n-type, <100>, 3–5 Ωcm, 78 mm × 78 mm, thickness 170 µm) double-side pyramidally textured by wet-chemical etching were used as substrates. The native silicon oxide was removed by a hydrofluoric acid dip. The ITO was deposited with DC magnetron sputtering of a 3% SnO_2-doped In_2O_3 rotating tube target at a heater temperature of 250 °C, 3×10^{-3} mbar operating pressure, 270 V DC bias voltage,

90 sccm Ar flow and 4.5 sccm O_2 flow. The substrates were laser cut in 26 mm × 39 mm pieces without protective resist coating, because it was previously obeserved that residues remained on the samples after resist stripping. Instead, the substrates were placed face-down on a glass plate during the laser cutting without protective resist coating followed by a cleaning procedure employing acetone, isopropyl alcohol and water to remove any organic contaminations. The samples were dried with a nitrogen gun, vacuum sealed and stored until further use.

Then metal was electroplated on samples employed for cross-sectional SEM imaging. Therefore, after electroplating, the samples were scratched with a diamond scriber and cleaved with cleaving pliers. Looking on the samples' cross-section, SEM pictures were taken under a 10° angle.

Samples used for pull-off tests or CTLM measurements were photolithographically structured with photoresist. Therefore, the samples were coated with HMDS at 135 °C, AZ 12XT-20PL-10 was spin-coated at 1500 rpm for 30 s and baked at 110 °C for 180 s. Optical lithography with a laser writer and a mask aligner was employed at a dose of 3000 mJ/cm^2 to facilitate the pull-off experiments, the CTLM measurements and to generate a 5 mm wide strip at the sample edge, which was used for measuring the front-side potential during electroplating, respectively. Afterwards, a post exposure bake was performed at 90 °C for 60 s and the photoresist was developed with AZ 826 MIF for 180 s. The corresponding masks are described in the sections "Pull-off Tests" and "CTLM Measurements". Electroplating was employed as an additive process to fill up the photoresist features.

Electroplating

The Fe electrolyte compounds were 60 g/l iron sulfate, 7 g/l ascorbic acid and 31 g/l boric acid. Fe electroplating was performed at 40 °C and pH 2.5–2.9 with a high-purity iron anode at a constant current density of 10 mA/cm^2 for 5 min. NB Semiplate Ni 100 was used as Ni electrolyte. Ni electroplating was performed at 40 °C and pH 2.9–3.2 with a platinum-coated

titanium grid anode at a constant voltage of 1.5 V, measured between the anode and the frontside-contact, for 3 min leading to a current starting at 4–5 mA/cm^2 and decreasing to 1–3 mA/cm^2 during the plating process. The voltage was set to a maximum of 1.5 V to limit the amount of hydrogen evolution on the cathode surface which is usually accompanied with adhesion problems. The Cu electrolyte contained 25 g/l copper pyrophosphate, 220 g/l potassium pyrophosphate, 9.7 g/l ammonium nitrate, 32.3 g/l ammonium oxalate hydrate. Before electroplating, the copper anode had been cleaned for a few minutes in sulfuric acid removing the native oxide from the surface. Cu electroplating was performed at 50 °C and pH 7.9–8.6 at a constant current density of 20 mA/cm^2 for 15 min. The Cu electrolyte composition and process conditions were adopted from Minsek [9].

The substrates are used as the cathode in the electroplating setup which is schematically shown in Figure 1. They were placed in a sample holder which is made out of a front-

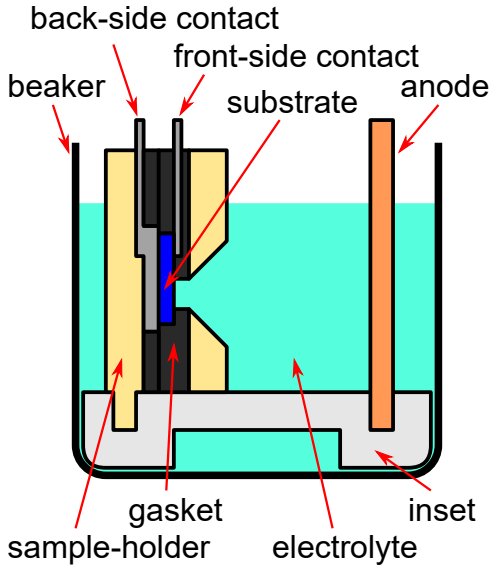

Figure 1: Schematic setup used for electroplating experiments.

and back-side part pressed together with screws to seal the sample with a gasket preventing intrusion of electrolyte. Then, the sample holder and the anode were immersed in an electrolyte filled in a 1000 ml glass beaker which was placed on a hotplate with temperature regulation and magnetic stirring while an inset kept the distance between the anode and the

cathode at around 40 mm. Moreover, the sample holder has got a 1 cm × 1 cm opening in the front-side part where the electrolyte was in contact with the substrate. Being connected to a power supply, the current was applied through the anode and a stainless-steel plate at the back-side of the substrate allowing a homogeneous current flow through the substrate while an inserted stainless-steel strip was used as a front-side contact to measure and regulate the plating voltage with respect to the anode potential. After the electroplating of each metal layer, the sample holder was thoroughly rinsed with DI water.

Pull-off Tests

The mask for pull-off tests has nine equally sized squares each with an area of 2 mm × 2 mm. They are arranged in a 3 by 3 array separated by 1 mm wide gaps. After metal electroplating of Fe/Ni/Cu layers, the force to pull off the metal layers from ITO-coated substrates was measured. To do so, a self-made setup was employed as shown in Figure 2. The back-side

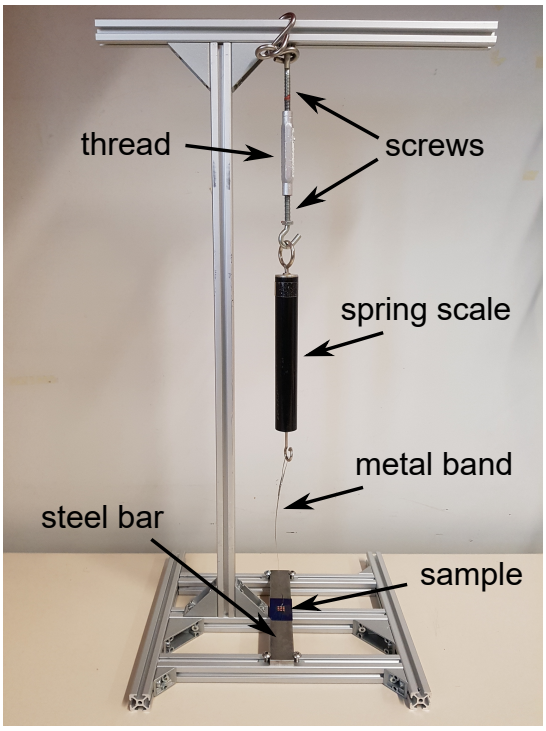

Figure 2: Self-made setup used for measuring the pull-off force of electroplated thin-films.

of the substrate was glued to an approximately 1 cm thick stainless-steel bar with two-

component glue. A 2 mm wide metal band was glued to the Cu surface of the metal layer on the front-side of the substrate with instant glue and the other side of the metal band was attached to a spring scale. By two counterrotating screws in one thread the spring scale was pulled upwards exerting a pulling force on the metal/ITO interface. The spring scale was filmed with a camera to record the maximum force at the exact moment when the metal layers were pulled off. The pull-off stress is calculated by dividing the pull-off force by the area of the electroplated metal.

CTLM Measurements

A schematic CTLM structure is shown in Figure 3 showing the inner and outer metal contacts in grey and defining the radius L and gap width d. A CTLM sample has multiple of these structures each with a different pair of gap width and radius with a size of 10–50 µm and 50–200 µm, respectively.

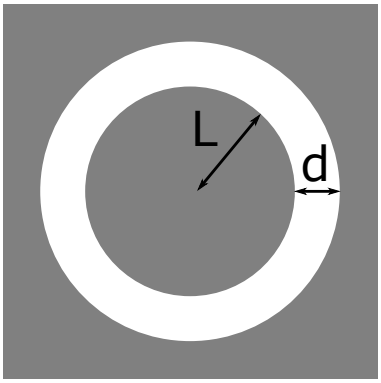

Figure 3: Schematic CTLM structure showing the inner and outer metal contacts in grey with the radius L of the inner circle and gap width d.

The CTLM structures were contacted to a parameter analyzer in 4-point configuration, that is two contact needles are placed on each contact, with a current range of ±1 mA and a current step of 0.05 mA. The current and voltage were recorded in order to use linear curve fitting to determine the resistance R_{T}.

The following equations model the electrical resistance R_T measured between the inner and outer contacts of a CTLM structure.[10] Assuming $L \gg 4L_\mathrm{T}$ and $L \gg d$ with L_T being the transfer length, the resistance is given by

$$R_\mathrm{T} = \frac{R_\mathrm{sh}}{2\pi L}\left(d + 2L_\mathrm{T}\right) C \tag{1}$$

with the sheet resistance R_sh, radius L, gap width d and a geometry dependent correction factor C:

$$C = \frac{L}{d}\ln\left(1 + \frac{d}{L}\right). \tag{2}$$

Normalization of the resistance gives an expression independent of the radius:

$$R = \frac{2\pi L}{C} R_\mathrm{T} \tag{3}$$

$$= R_\mathrm{sh} d + 2R_\mathrm{C} \tag{4}$$

with the contact resistance

$$R_\mathrm{C} = R_\mathrm{sh} L_\mathrm{T}. \tag{5}$$

As can be seen, the normalized resistance is linearly dependent on the gap width d. Thus, the sheet resistance, contact resistance and transfer length can be determined by linear curve fitting with equations 4 and 5.

The current density from the sheet into the contact is not uniformly distributed and instead it is exponentially decreasing under the contact area in dependence on the specific contact resistivity ρ_C and the sheet resistance R_sh. In fact, the transfer length L_T describes the characteristic distance to the contact edge where $1 - \mathrm{e}^{-1} \approx 63.2\,\%$ of the current has entered the contact and it is given by

$$L_\mathrm{T} = \sqrt{\frac{\rho_\mathrm{C}}{R_\mathrm{sh}}}. \tag{6}$$

Hence, the contact resistivity can be calculated by

$$\rho_{\mathrm{C}} = L_{\mathrm{T}}^2 R_{\mathrm{sh}} = \frac{R_{\mathrm{C}}^2}{R_{\mathrm{sh}}}. \tag{7}$$

Results

The SEM micrograph in Figure 4a shows the cross-section of an ITO-coated pyramidally textured Si substrate. The ITO layer is around 80 nm thin, conformally deposited on the pyramids and has a smooth surface. Figure 4b displays the nucleation process with many small grains of Fe on the surface of the ITO after electroplating at 10 mA/cm^2 for 10 s. The grains are mostly distributed evenly across the surface. Areas with fewer grains might indicate possible lifting or hydrogen formation preventing Fe deposition.

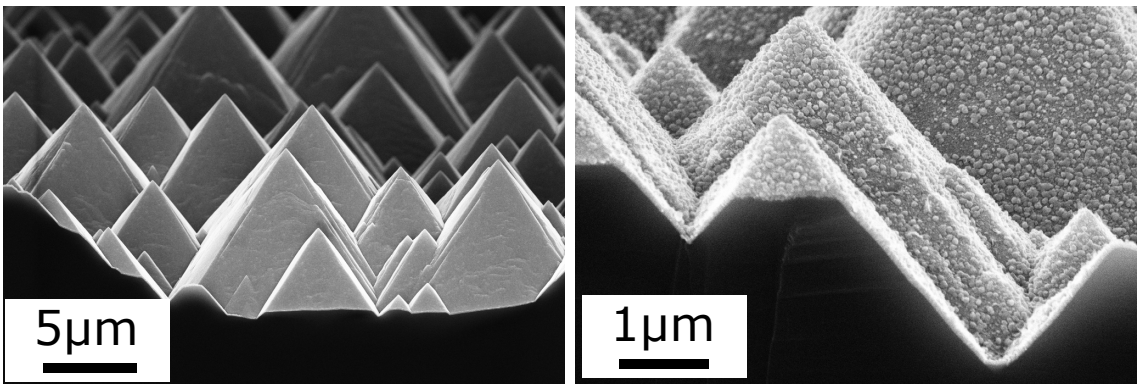

(a) (b)

Figure 4: SEM micrographs of ITO-coated pyramidally textured Si substrates before (a) and after (b) electroplating showing the nucleation after 10 s of Fe electroplating at 10 mA/cm^2.

Figure 5 depicts SEM micrographs of the cross-section of several samples with the consecutive electrodeposition of Fe, Ni and Cu on ITO-coated Si substrates. As illustrated in Figure 5a, the approximately 440 nm thin Fe layer exhibits dendritic, partially porous growth and a rough surface. Figure 5b shows that the surface is much smoother after subsequent Ni deposition on the Fe layer. Possible holes in the Fe layer are filled and closed by the approximately 100 nm thin Ni layer. However, it is hard to clearly distinguish the Ni and

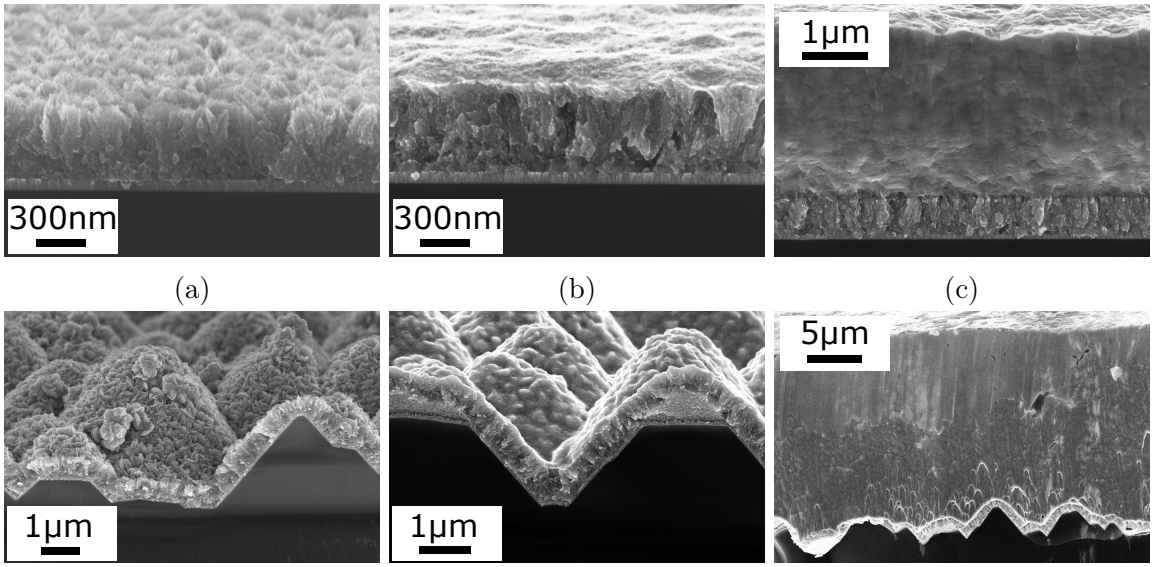

Figure 5: SEM micrographs of the breaking edge of electrodeposited Fe (a, d), Fe/Ni (b, e), Fe/Ni/Cu (c, f) on ITO-coated polished (a, b, c) or pyramidally textured (d, e, f) Si substrates. Deposition parameters were 10 mA/cm^2, 5 min for Fe, 1.5 V, 3 min for Ni and 20 mA/cm^2, 15 min (60 min on pyramidally texutred sample) for Cu.

Fe layers from each other. Figure 5c shows a 2.6 µm thick Cu layer deposited on the Fe/Ni layer. As shown in Figure 5d and 5e, the Fe and Ni layers conformally coat the pyramidally textured substrates and their layer thicknesses measured perpendicular to the pyramid surface were approximately 530 nm and 80 nm for Fe and Ni layers, respectively. The Cu layer in Figure 5f was deposited for 60 min, four times longer than in the case of the sample in Figure 5c, and is 15 µm thick. Many samples show excellent adhesion between Fe and ITO. However, cracks and partial lifting were sometimes observed at the Fe/ITO interface on pyramidally textured samples.

The Cu electroplating had also been tested directly on the Fe layer. Figure 6 shows the cross-section of a sample with Fe/Cu layer. Fe and Cu electroplating were performed at 10 mA/cm^2 for 2 min and 20 mA/cm^2 for 15 min, respectively. The metal layer exhibits poor adhesion and lifts from the substrate. The reason for this is uncertain.

The electroplated Fe/Ni/Cu metal stack on ITO withstood the scotch tape test and the adhesion strength was measured via pull-off tests. The pull-off stress for the two substrate

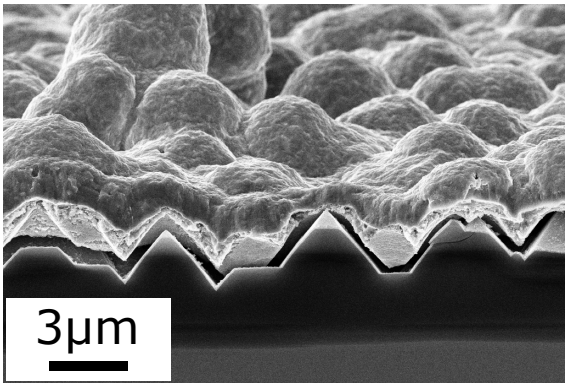

Figure 6: SEM micrograph of an ITO-coated pyramidally textured Si substrate with electroplated Fe/Cu layer showing poor adhesion and lifting of the metal layer. Electroplating was performed at 10 mA/cm^2 for 2 min and 20 mA/cm^2 for 15 min for Fe and Cu, respectively.

types is depicted in Figure 7. In total 61 metal stacks (37 on polished substrates and 24 on pyramidally textured substrates) were successfully pulled off and the average pull-off stress is 1.44 ± 0.97 MPa and 1.28 ± 0.38 MPa for polished and pyramidally textured substrates, respectively, with the given uncertainties being one standard deviation. Both substrate types yield approximately the same average pull-off force but for polished substrates the variance of the pull-off stress is much bigger with some large outliers (red crosses). The data points are also not normally distributed. The metal/ITO interface did often not break and instead chunks were torn from the Si substrate itself due to the applied pulling forces. Therefore, the measured values varied significantly and the given average values represent a lower bound for the actual average Fe/ITO interface adhesion strength.

CTLM structures were used to determine the contact resistivity, sheet resistance and transfer length of the Fe/Ni/Cu metal contact on ITO-coated Si substrate. Figure 8a shows the top view of a CTLM structure with a nominal inner radius of 200 µm and a nominal gap width of 15 µm. However, remeasuring the gap width in Figure 8b reveals a value of only 12.1 µm. The gap width was therefore measured for all CTLM structures and they are around 3 µm smaller than the nominal values of the mask. This might have been caused by an overdevelopment of the exposed photoresist. This error was taken into account by measuring the dimensions of each structure with SEM.

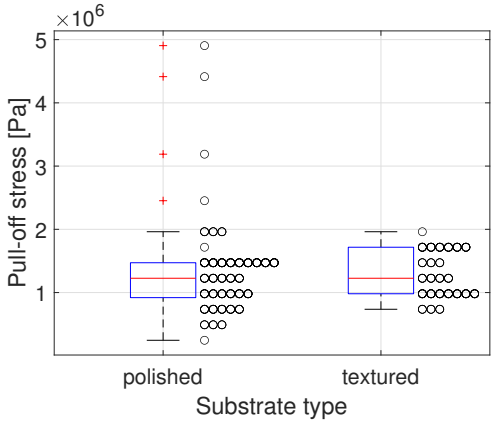

Figure 7: Pull-off stress of electroplated Fe/Ni/Cu metal stacks on ITO-coated polished or pyramidally textured silicon substrates. The plot shows the median (red line), the upper and lower interquartile (blue box) and the maximum/minimum values (whiskers) excluding the outliers (red plus symbols). Outliers are defined as values which are more than 1.5 times the interquartile range away from the top or bottom of the box. The values of the single measurements are shown as black circles.

Figure 9 shows the normalized and corrected resistance R in dependence of the gap width d of the CTLM structures. Linear curve fittings yield contact resistivities ρ_C of $6.5 \times 10^{-7}\,\Omega\,\mathrm{cm}^2$ and $9.0 \times 10^{-7}\,\Omega\,\mathrm{cm}^2$, sheet resistances R_{sh} of $275\,\Omega/\square$ and $174\,\Omega/\square$ with transfer lengths L_T of 487 nm and 720 nm for polished and pyramidally textured substrates, respectively.

Discussion

Before using Fe electroplating, preliminary experiments with direct Cu and Ni electroplating tests exhibited poor adhesion on ITO as can be observed in Figure 10. Ni was electroplated at 1 V for 5 min but after breaking the sample for SEM investigation the Ni layer lifts from the ITO. In case of Cu electroplating on ITO, process-steps, like rinsing with water, lifted the Cu layer from ITO. These Cu and Ni layers were easily pulled-off by scotch-tape method.

The results of this study show that Fe electroplating from an acidic iron sulfate electrolyte deposits adherent layers on ITO. This was expected based on previous findings using a reducing agent to deposit Fe on ITO.[7] The hypothesis that the strong adhesion is attributed

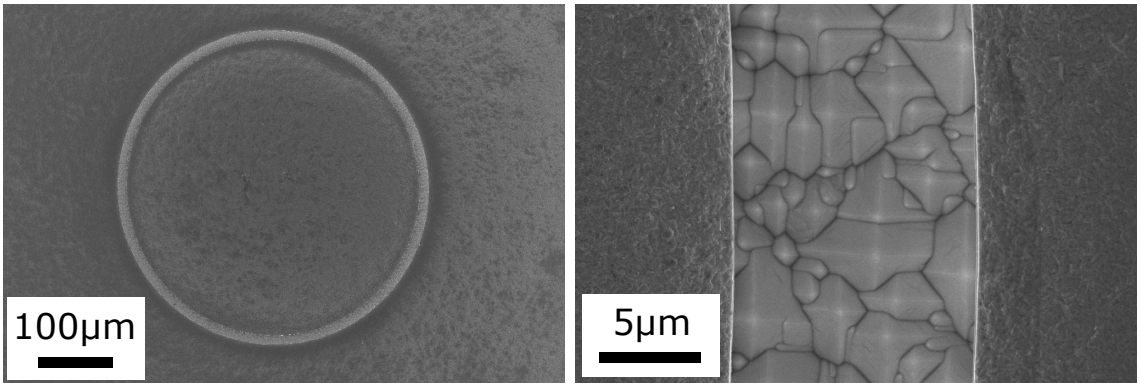

(a) (b)

Figure 8: Top view of CTLM structure with electroplated Fe/Ni/Cu metal contacts on ITO-coated Si substrate: (a) overview image, (b) zoomed image showing the gap with ITO-coated pyramids in the center.

to the formation of strongly bonded iron oxide at the interface to ITO[9] is not clear yet. The adhesion is strong enough to sustain the scotch tape test and mostly maintained adherent after breaking the sample as observed by an SEM. These micrographs show excellent adhesion at the Fe/ITO interface for polished substrates. Although the adhesion was mostly good also for pyramidally textured substrates, some areas still have shown partial lifting of the Fe from ITO. A difference in adhesion strength was observed for the two substrate types where the average pull-off stress for polished substrates is a little bit higher but its variance was much higher compared to pyramidally textured substrates. On the pyramidally textured substrates the field gradient of the pulling force with respect to the pyramid surface is different than for the polished substrate. However, the Cu electroplating bath has a high throwing power and uniform layer thickness is therefore achieved. Thus, the field gradient of the pulling force might not be the reason. The lifting was often observed in the Si substrate itself or at the ITO/Si interface suggesting that the adhesion is improved compared to direct Cu electroplating on ITO and that the measured pull-off stress might not even depend on the ITO/metal interface.

The pull-off forces were applied vertical to the samples. On polished substrates this means that the force components are perpendicular to the surface. However, due to the pyramidal

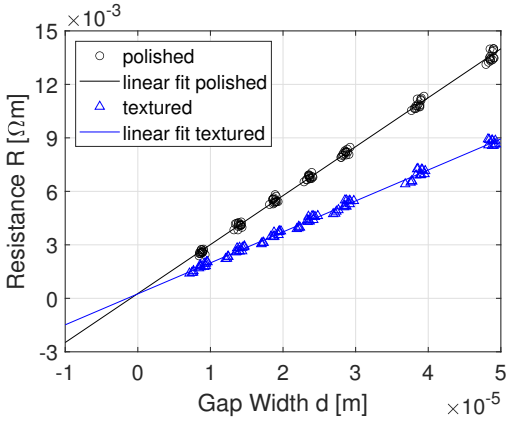

Figure 9: Normalized resistance R of CTLM structures of Fe/Ni/Cu contacts on ITO-coated Si substrate in dependence of the gap width d and the type of surface texturization. Linear curve fittings yield sheet resistances R_{sh} of $275\,\Omega/\square$ and $174\,\Omega/\square$, contact resistances R_{C} of $1.34 \times 10^{-4}\,\Omega\mathrm{m}$ and $1.25 \times 10^{-4}\,\Omega\mathrm{m}$ and transfer lengths L_{T} of 487 nm and 720 nm for polished and pyramidally structured substrates, respectively.

texturization, these forces also have components in parallel to the pyramid surfaces which might decrease the pull-off stress. In general, the pyramid geometry may also affect the layer growth due to a higher effective surface area or inhomogeneously confined electrical fields at the tips of the pyramids and the valleys in between them possibly changing the nucleation process or inducing additional layer stress. However, the field gradient might not be responsible

Due to the good adhesion of the Fe, it can be used as an intermediate layer for subsequent electroplating to heighten the layer thickness and reduce sheet resistance of the metal contacts. In our experiments, direct Cu electroplating on the Fe layer has not led to adherent metal stacks and was therefore not further investigated. However, when a thin conformal Ni layer was deposited between Fe and Cu, the Fe/Ni/Cu layer stack maintained adherent even for a Cu layer thickness of 15 µm. The Cu might induce layer stress due to its higher lattice constant than Fe. Although the Ni lattice constant is only a little bit smaller than the lattice constant of Cu, this might be enough to reduce the layer stress. In addition, Cu electrolyte might reach the ITO surface facilitated by the porosity of the Fe layer. Then, due to the higher redox potential of Cu compared to Fe, Cu replaces the Fe at the Fe/ITO

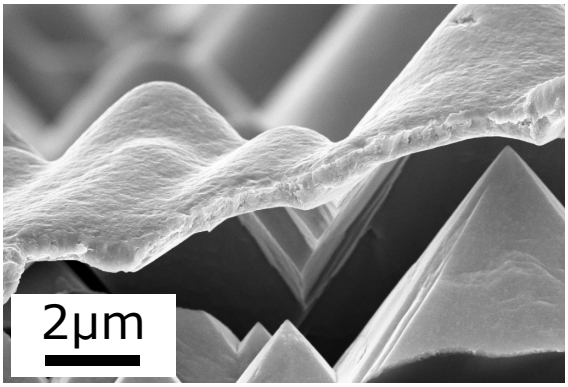

Figure 10: SEM micrograph of an ITO-coated pyramidally textured Si substrate with electroplated Ni layer showing poor adhesion and lifting of the metal layer. Electroplating was performed at 1 V for 5 min.

interface and hence leads to the bad adhesion already known from the preliminary Cu/ITO experiments. These pores are filled through the addition of the conformal Ni layer preventing the Cu electrolyte to reach the Fe/ITO interface.

The CTLM measurements of Fe/Ni/Cu metal stack contacts on ITO have shown low contact resistivities. Assuming the Fe/Ni and Ni/Cu interfaces have much lower contact resistivities and the bulk resistances are negligible, the determined contact resistivities should mostly apply to the Fe/ITO interface. The lowest contact resistivities of electroplated metal contacts on ITO reported previously by Lee et al.[8] were made by co-deposition of Cu-Ni and measured with transmission line model (TLM) structures having a contact resistivity of $3.3 \times 10^{-5}\,\Omega\,\mathrm{cm}^2$. Nghiem et al.[11] deposited Au and Ni on ITO with a not further specified deposition technique and investigated the contacts with CTLM measurements (radius: 75 µm) reporting contact resistances of $0.03\,\Omega$ (ITO sheet resistance: $48\,\Omega/\square$) for Au/ITO and even lower values for Ni/ITO. After normalization of the contact resistance, the contact resistivity is calculated with equation 7 to be around $4.2 \times 10^{-8}\,\Omega\,\mathrm{cm}^2$. The authors pointed out that the measurement precision suffered from measurement device errors and the influence of needle positioning on the CTLM structures. They estimate a total error of $0.1\,\Omega$ which is above the range of their measured contact resistances. It was concluded that CTLM measurements might not be applicable to precisely measure a small contact resistance

which scales inversely with the relatively large effective contact width which is equal to the circumference of the inner metal contact circle which cannot be scaled down indefinitely due to the constraint of $L \gg 4L_{\mathrm{T}}$ with the radius L and the transfer length L_{T}. It was suggested to use TLM structures instead where contact width can be scaled down more easily but the fabrication is more complex due to additional mesa etching of ITO. However, a study of Yu et al.[12] suggests that CTLM measurements are still applicable having contact resistivity errors around $5 \times 10^{-9}\,\Omega\,\mathrm{cm}^2$.

Conclusions

Fe electroplating was used to deposit adherent layers on ITO-coated polished or pyramidally textured Si substrates. In order to reduce metal sheet resistance, the metal layer can be thickened by further electroplating. This was shown by subsequent Fe, Ni and Cu electroplating creating a multi-layer metal stack on ITO. The adhesion of such multi-layers was tested by scotch tape method and the pull-off force perpendicular to the substrate was measured. Pyramidally textured substrates had a lower pull-off force. CTLM structures were fabricated made from the Fe/Ni/Cu multi-layer on ITO and the measurements exhibit low contact resistivities. To the best of our knowledge, this is the lowest reported contact resistivity for electroplated metal contacts on ITO.

Acknowledgement

We thank Dr. Oleksandr Astakhov (FZJ, IEK-5) for supporting measurements and ITO depositions. This work was funded by the Bundesministerium für Wirtschaft und Energie (BMWi) in the network project “PATOS” (FKZ 0324074E).

References

(1) Liu, J. S.; Laverty, S. J.; Maguire, P.; McLaughlin, J.; Molloy, J. *Journal of The Electrochemical Society* **1994**, *141*, L38–L40.

(2) Kim, J. J.; Cha, S. H. *Japanese Journal of Applied Physics* **2002**, *41*, L1269–L1271.

(3) Hau, N. Y.; Chang, Y.-H.; Huang, Y.-T.; Wei, T.-C.; Feng, S.-P. *Langmuir : the ACS journal of surfaces and colloids* **2014**, *30*, 132–139.

(4) Lee, S. H.; Lee, D. W.; Lee, S. H.; Park, C. K.; Lim, K. J.; Shin, W. S. *Japanese Journal of Applied Physics* **2018**, *57*, 08RB13.

(5) Lee, S. H.; Lee, D. W.; Kim, H. J.; Lee, A. R.; Lee, S. H.; Lim, K.-j.; Shin, W.-s. *Materials Science in Semiconductor Processing* **2018**, *87*, 19–23.

(6) Lee, S. H.; Lee, D. W.; Lee, A. R.; Kim, H. J.; Lee, S. H. *Journal of the Korean Physical Society* **2018**, *72*, 469–475.

(7) Ahmet, I. Y.; van de Krol Roel,; Abdi, F. F.; Ma, Y. Verfahren zur Oberflächenbehandlung einer Probe die mindestens eine Oberfläche eines Metalloxids aufweist und Metalloxid mit behandelter Oberfläche. 2019.

(8) Lee, S. H.; Lee, D. W.; Lim, K.-j.; Shin, W.-s.; Kim, J. *Electronic Materials Letters* **2019**, *15*, 314–322.

(9) Minsek, D. W. Electroplating of metals on conductive oxide substrates: United States Patent. 2017.

(10) Schroder, D. K. *Semiconductor material and device characterization*, third edition ed.; Wiley-Interscience: Hoboken, NJ, 2006.

(11) Nghiem, G. M.; Kristiansen, H.; Aasmundtveit, K. Investigation of contacts between metal and transparent conductive oxides. 2016 6th Electronic System-Integration Technology Conference (ESTC). Piscataway, NJ, 2016; pp 1–4.

(12) Yu, H.; Schaekers, M.; Schram, T.; Rosseel, E.; Martens, K.; Demuynck, S.; Horiguchi, N.; Barla, K.; Collaert, N.; de Meyer, K.; Thean, A. *IEEE Electron Device Letters* **2015**, *36*, 600–602.